



A multicenter study on the preoperative prediction of gastric cancer microsatellite instability status based on computed tomography radiomics

Xiuqun Liang¹ · Yinbo Wu² · Ying Liu¹ · Danping Yu³ · Chencui Huang⁴ · Zhi Li³

Received: 7 February 2022 / Revised: 21 March 2022 / Accepted: 22 March 2022 / Published online: 7 April 2022
© The Author(s), under exclusive licence to Springer Science+Business Media, LLC, part of Springer Nature 2022

Abstract

Purpose To construct and validate a radiomics feature model based on computed tomography (CT) images and clinical characteristics to predict the microsatellite instability (MSI) status of gastric cancer patients before surgery.

Methods We retrospectively collected the upper abdominal or the entire abdominal-enhanced CT scans of 189 gastric cancer patients before surgery. The patients underwent postoperative gastric cancer MSI status testing, and the dates of their radiologic images and clinicopathological data were from January 2015 to August 2021. These 189 patients were divided into a training set ($n=90$) and an external validation set ($n=99$). The patients were divided by MSI status into the MSI-high (H) arm (30 and 33 patients in the training set and external validation set, respectively) and MSI-low/stable (L/S) arm (60 and 66 patients in the training set and external validation set, respectively). In the training set, the clinical characteristics and tumor radiologic characteristics of the patients were extracted, and the tenfold cross-validation method was used for internal validation of the training set. The external validation set was used to assess its generalized performance. A receiver-operating characteristic (ROC) curve was plotted to assess the model performance, and the area under the curve (AUC) was calculated.

Results The AUC of the radiomics model in the training set and external validation set was 0.8228 [95% confidence interval (CI) 0.7355–0.9101] and 0.7603 [95% CI 0.6625–0.8581], respectively, showing that the constructed radiomics model exhibited satisfactory generalization capabilities. The accuracy, sensitivity, and specificity of the training dataset were 0.72, 0.63, and 0.77, respectively. The accuracy, sensitivity, and specificity of the external validation dataset were 0.67, 0.79, and 0.60, respectively. Statistical analysis was carried out on the clinical data, and there was statistical significance for the tumor site and age ($p < 0.05$). MSI-H gastric cancer was mostly seen in the gastric antrum and older patients.

Conclusions Radiomics markers based on CT images and clinical characteristics have the potential to be a non-invasive auxiliary diagnostic tool for preoperative assessment of gastric cancer MSI status, and they can aid in clinical decision-making and improve patient outcomes.

✉ Zhi Li
lz85920@zju.edu.cn

¹ Department of Radiology, The People's Hospital of Guangxi Zhuang Autonomous Region & Research Center of Radiology, Guangxi Academy of Medical Sciences, Nanning 530021, Guangxi, China

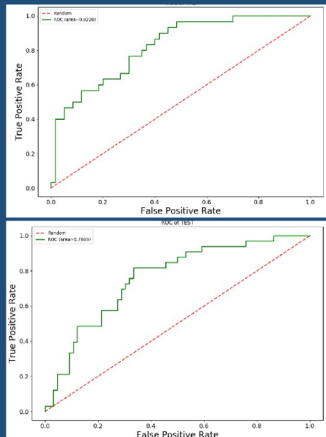
² Department of Radiology, Cancer Center, Zhejiang Provincial People's Hospital, Affiliated People's Hospital, Hangzhou Medical College, Hangzhou 310014, Zhejiang, China

³ Department of Radiology, First Affiliated Hospital, School of Medicine, Zhejiang University, Hangzhou 310007, Zhejiang, China

⁴ Department of Research Collaboration, R&D center, Beijing Deepwise & League of PHD Technology Co, Ltd, Beijing 100080, China

Graphical abstract

A multicenter study on the preoperative prediction of gastric cancer microsatellite instability status based on computed tomography radiomics Abstract



Evaluation of model performance:

- AUC of radiomics model in the training set: 0.8228 [95% CI: 0.7355–0.9101]
- AUC of radiomics model in external validation set: 0.7603 [95% CI: 0.6625–0.8581]

Xiuqun Liang et al; 2022 DOI:

Abdominal Radiology
The Official Journal of the Society of Abdominal Radiology www.abdominalradiology.org

Keywords Microsatellite instability · CT · Radiomics · Gastric cancer

Abbreviations

MSI	Microsatellite instability
CT	Computed tomography
AUC	Area under the curve
ROC	Receiver operating curve
NCCN	National comprehensive cancer network
MMR	Mismatch repair
MSI-H	MSI-high frequency
MSI-L	MSI-low frequency
MSS	MSI stability
VOI	Volume of interest
ROI	Region of interest
DNA	Deoxyribonucleic acid
FDA	Food and Drug Administration
GLCM	Gray-level co-occurrence matrix
GLRLM	Gray-level run length matrix
GLSZM	Gray-level size zone matrix
GLDM	Gray-level dependence matrix
NGTDM	Neighborhood gray-tone difference matrix

Introduction

Based on 2020 global data statistics, the incidence and mortality rate of gastric cancer in men are ranked 4th among all cancers, and the incidence and mortality rate of gastric cancer in women is ranked 7th and 5th, respectively [1]. Gastric cancer can be defined by molecular subtypes, which can be used to predict outcomes and guide targeted therapies [2].

Approximately 15–25% of gastric cancer patients have the unique molecular phenotype of microsatellite instability (MSI) [3]. MSI is characterized by alterations in length within short-repeated DNA sequences, resulting from mutational inactivation or epigenetic silencing of DNA mismatch repair genes [4]. Studies showed that MSI is a predictor of sensitivity to immunotherapy [5, 6] and enables some patients to benefit from immunotherapy [7, 8] but not from conventional chemotherapy [9–11]. In addition, the US Food and Drug Administration (FDA) announced in 2017 that the monoclonal antibody drug pembrolizumab can be used for the treatment of MSI-H or DNA mismatch repair-deficient marker-positive tumors and unresectable and metastatic tumors. The NCCN Gastric Cancer Guidelines, Version 4.2021, recommend that MSI status should be

routinely tested in patients who are newly diagnosed with gastric cancer.

Currently, immunohistochemical staining or molecular biology tests are predominantly used to determine the gastric cancer MSI status in clinical practice [12]. The samples used for these test methods can only be obtained via preoperative biopsy or postoperative pathological samples. However, the temporal heterogeneity [13] of MSI status in tumor tissues at different stages and over the course of treatment has curtailed the use of many histological methods. Furthermore, contraindications to endoscopy or surgery, as well as severe complications caused by endoscopy [14], unqualified specimens [15], and unnecessary biopsy for metastatic patients will all hinder histological examinations. Therefore, the development of a relatively non-invasive and convenient alternative biomarker to predict gastric cancer MSI status may contribute to accurate treatment.

Radiomics can be used to mine high-throughput quantitative imaging features and has the potential for quantitation of intratumor and intertumor heterogeneity [16]. Recent studies showed that radiomics is widely used in oncology studies, and researchers have demonstrated some clinical application value [17–19]. Radiomics studies on tumor MSI status have also been reported [20–24]. These reports demonstrated the feasibility of using radiomics to analyze tumor MSI status. Thus far, no radiomics studies on MSI status detection in

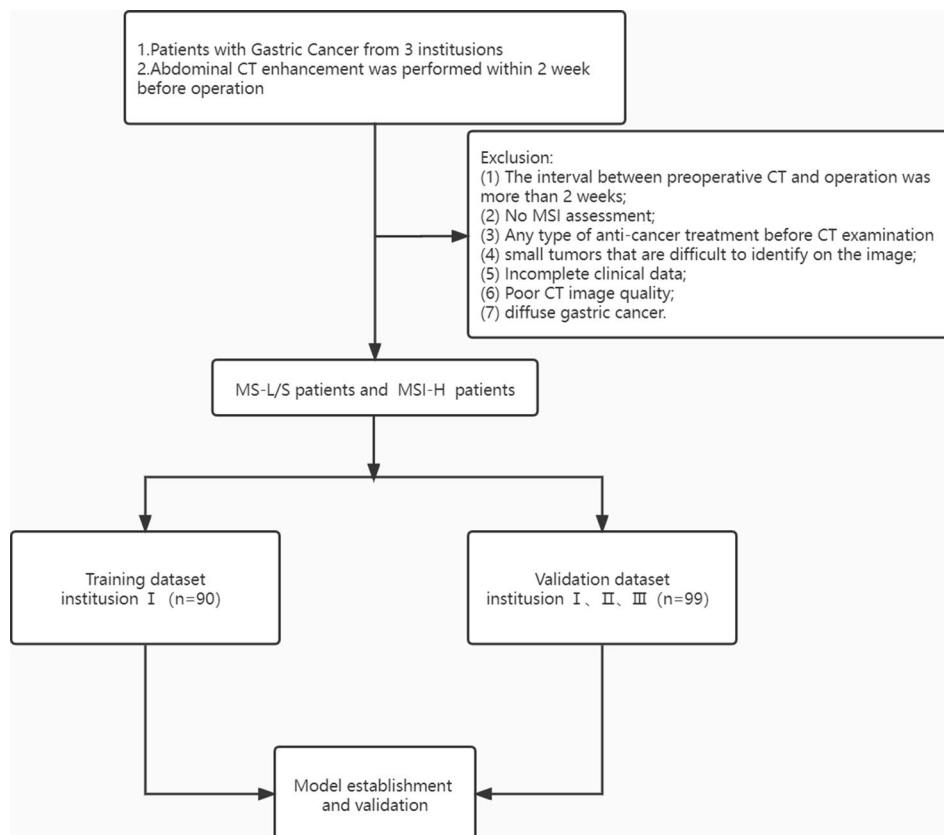
gastric cancer have been performed. In this study, preoperative-enhanced computed tomography (CT) images and clinical characteristics were used to construct and validate a radiomics model for predicting gastric cancer MSI status.

Materials and methods

Patients

This retrospective study was approved by the institutional review committee of Zhejiang Provincial People's Hospital (institution I), the First Affiliated Hospital of Zhejiang University School of Medicine (institution II), and The People's Hospital of Guangxi Zhuang Autonomous Region (institution III). The signed informed consent was abandoned. The study was conducted in accordance with the declaration of Helsinki. Patients in three participating institutions who underwent a preoperative-enhanced CT scan and were histopathologically proven to have gastric adenocarcinoma were enrolled in the study. Figure 1 shows the patient selection and exclusion process. The exclusion criteria are as follows: (1) The interval between preoperative CT and operation was more than 2 weeks; (2) No MSI assessment; (3) Any type of anti-cancer treatment, such as radiotherapy, chemotherapy, or biotherapy before CT examination; (4) Small tumors that

Fig. 1 Flowchart of the patient selection and patient exclusion



are difficult to identify on the image; (5) Incomplete clinical data; (6) Poor CT image quality; and (7) Diffusive gastric cancer. Finally, 189 patients were retrospectively included in this study, in which the clinical data were retrospectively analyzed. The clinical characteristics of patients were recorded, including age, gender, tumor site (gastric cardia-fundus, gastric body, and gastric antrum), carcinoembryonic antigen (CEA) status (normal or abnormal), and serum tumor marker carbohydrate antigen-199 (CA199) status (normal or abnormal).

MSI status assessment

In this study, the expression levels of protein products of the MMR gene (MLH1, MSH2, MSH6, and PMS2) were measured, and immunohistochemical staining was used to measure MSI status. Immunohistochemical staining results were interpreted by two pathologists with more than 10 years of experience in diagnosing abdominal tumors, and both pathologists agreed on the results. Patients were divided into two groups, with the MSI-L/S group containing patients whose 4 MMR proteins were all positive, while the MSI-H group included patients with any MMR protein that was negative.

CT image collection

All of the patients underwent upper abdominal or the entire abdominal-enhanced CT examination 2 weeks before surgery. Before the CT examination, patients were asked to drink 800–1000 ml water in 15–20 min. Seven different CT scanners from 3 institutions were used to acquire CT images. Two CT scanners were used in institution I, including a 64-slice CT scanner and a 128-slice CT scanner (Siemens Healthineers). Three CT scanners were used in institution

II, including a 64-slice and a 256-slice CT scanner (Philips Healthcare) and a 16-slice CT scanner (Toshiba Medical System). In institution III, a 64-slice CT scanner (Siemens Healthineers) and a 256-slice CT scanner (Philips Healthcare) were used. The mean acquisition parameters of the 3 institutions were tube voltage: 120 keV (100–130 keV), tube current: 213 mAs (125–300 mAs), interval: 0.6–1.25 mm, and slice thickness: 3–7 mm. A high-pressure injector was used to inject the contrast agent (2 mL/kg) (Jiangsu Hengrui Pharmaceuticals Co. Ltd.) at a speed of 2.5–3.5 mL/s. After injection, the trigger threshold was 140–160 HU, and CT scans were performed at the arterial phase and portal venous phase, with 6–10 s and 40–45 s delays, respectively, after the threshold value.

Tumor segmentation

A picture archiving and communication system workstation was used to export arterial phase and portal venous phase CT images in the DICOM format. Two radiologists with 8 and 10 years of experience in abdominal imaging used the ITK-SNAP image-processing software (version 3.8.0, www.itksnap.org) to manually delineate the volume of interest at the axial position, continuously delineate the region of interest (ROI) from the slice where the lesion began, and perform segmentation along the tumor contour. The ROI included intratumor necrotic or hemorrhagic regions; normal gastric walls, neighboring adipose tissues, and gastric contents were avoided as much as possible (Fig. 2). After 1 week, the radiologist with 8 years of experience performed delineation again in all of the patients to assess intra-observer and inter-observer feature extraction consistency. SPSS software was used for inter-group and intra-group correlation coefficient (ICC) analysis. Satisfactory consistency was defined by an ICC > 0.75. Only radiomics features with

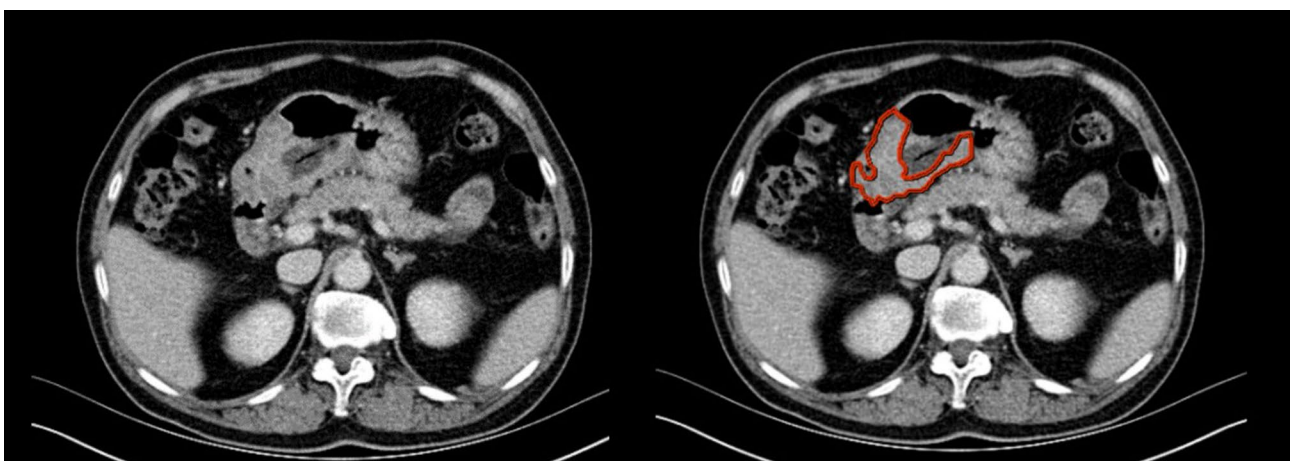


Fig. 2 A 70-year-old female gastric cancer patient. The region within the red line in the right figure indicates the ROI of the tumor

satisfactory reproducibility ($ICC > 0.75$) were selected for further analysis.

Radiomics analysis

This study used the Dr. Wise Multimodal Research Platform (<https://keyan.deepwise.com>, V1.6.2) (Beijing Deepwise & League of PHD Technology Co., Ltd., Beijing, China) for radiomics analysis, including image annotation, feature extraction and selection, and modeling. Figure 3 shows the radiomics analysis procedure.

Image preprocessing

B-spline interpolation sampling was used for resampling of images with different resolutions. After resampling, the same resolution was obtained for all of the samples, and the grayscale image was standardized.

Feature extraction

Radiomics features were extracted from the original images and pre-processed images. From every ROI, 4032 radiomics features (Table 1) were extracted, including first-order features, shape features that describe tumor morphology, gray-level co-occurrence matrix (GLCM), gray-level run length

matrix (GLRLM), gray-level size zone matrix (GLSZM), gray-level dependence matrix (GLDM), and neighborhood gray-tone difference matrix (NGTDM) features that describe the texture of the tumor interior and surface. Then, Z-score standardization (i.e., subtraction of the mean followed by division with the standard deviation) was performed. Statistical analysis was carried out on the clinical data, and two clinical characteristics (tumor site and age) exhibited statistical significance ($P < 0.05$). These two clinical characteristics and the extracted radiomics features were included as radiomics characteristics for analysis.

Feature dimensionality reduction and model construction

Feature correlation analysis was carried out to identify radiomics features. When the linear correlation coefficient of two features was above a certain threshold (linear correlation coefficient threshold = 0.9), the variable with the lowest effect on the dependent variable was removed. Finally, 20 features were included in the model. The logistic regression classification algorithm was used to construct a radiomics model based on the selected features. After the model was constructed, the tenfold cross-validation method was used for internal validation of the training set. All of the data were divided into 10 parts, and 9 parts were used for model

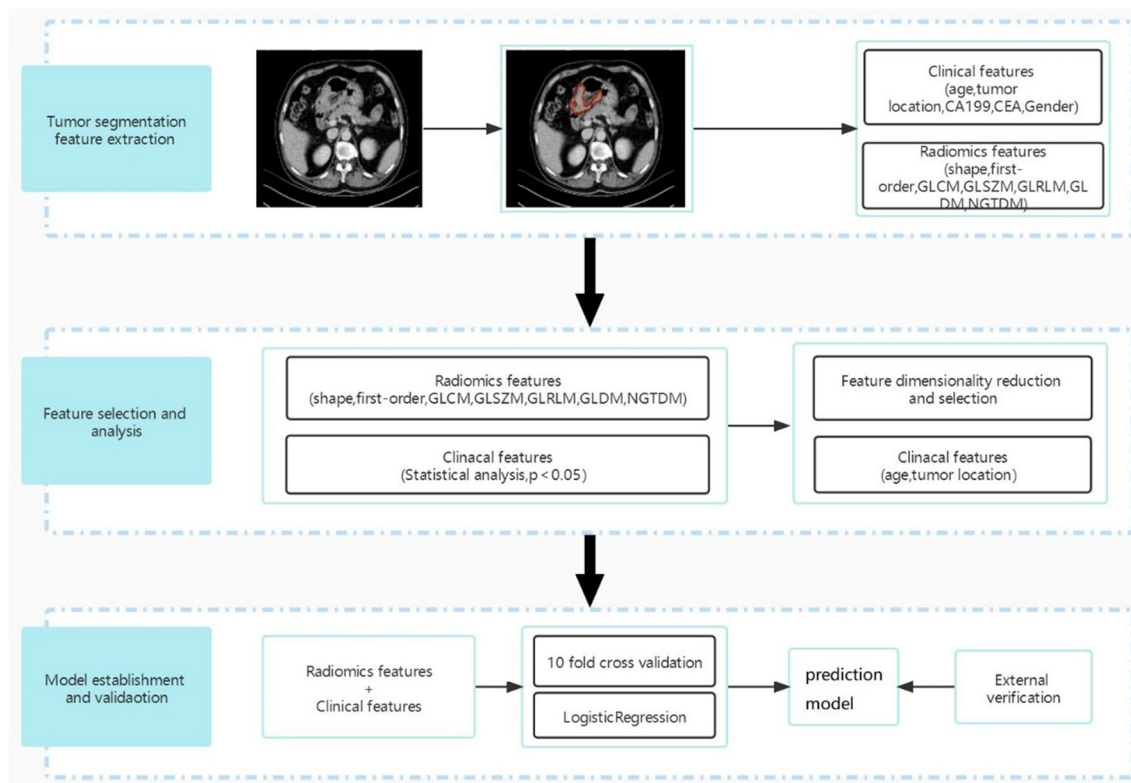
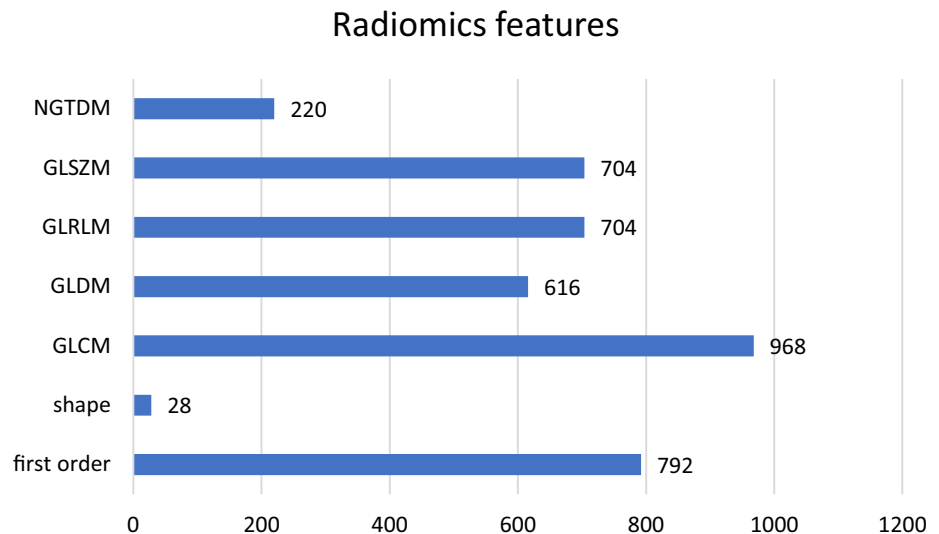


Fig. 3 The radiomics analysis framework in this study

Table 1 Extracted radiomics features

training, while 1 part was used to assess the model effectiveness. After the training and internal validation were performed, the mean of the 10 tests was used to assess model performance. Finally, the external validation set was used to assess the generalization capabilities of the model. The receiver-operating characteristic (ROC) curve was plotted to assess the model performance. The assessment markers mainly included the area under the curve (AUC), sensitivity, specificity, and accuracy. The AUC was the main assessment marker used for model performance.

Statistical analysis

Descriptive statistics were used to analyze the clinical data in the training and validation sets. The independent samples' *t* test was used for comparison of numerical data (age), and the chi-square test was used for comparison of categorical data (gender, tumor site, CEA status, and CA199 status). A difference with $p < 0.05$ was considered to be statistically significant. SPSS (IBM SPSS Statistics 26.0) software was used for all of the statistical analyses.

Results

Clinical characteristics

In the current study, 189 gastric adenocarcinoma patients in 3 institutions were included based on the exclusion criteria. There were 63 MSI-H gastric cancer patients, of which 31 were from institution I, and 32 were from institutions II and III. There were 126 MSI-L/S gastric cancer patients, of which 68 were from institution I, and 58 were from institutions II and III. There were 140 males and 49 females (mean age: 66 years, age range: 31–90 years). For model design

prediction, 90 patients from institution I were used as the training dataset, and the remaining 99 patients from the 3 institutions were used as the external validation dataset.

Table 2 shows the clinical characteristics of the gastric cancer patients. The results showed that there was statistical significance ($p < 0.05$) associated with the tumor site in the training and external validation sets, because MSI-H gastric cancer mostly occurs in the gastric antrum. In the training set, the age of diagnosis of the MSI-H group was higher than that of the MSI-L/S group ($p < 0.05$).

Radiomics feature analysis results

After feature dimensionality reduction, 20 clinical and radiomic characteristics were included in the model, of which 12 radiologic features were extracted from the arterial phase, including 4 first-order features (maximum, skewness, kurtosis, 90th percentile), 5 GLSZM (Size Zone Non-Uniformity Normalized, Size Zone Non-Uniformity, Small Area High Gray-Level Emphasis, Small Area Low Gray-Level Emphasis, and Small Area Emphasis), 1 GLDM (Dependence Entropy), 1 NGTDM (Busyness), 1 GLCM (Informational Measure of Correlation 2); and 7 radiologic features were extracted from the portal venous phase, including 1 shape feature (Maximum 2D Diameter Slice), 3 GLSZM (Gray-Level Non-Uniformity, Gray-Level Variance, Gray-Level Non-Uniformity), 1 GLDM (Dependence Variance), 2 GLCM (Informational Measure of Correlation 2, Cluster Shade), 1 GLRLM (Short Run Emphasis), and 1 clinical characteristic (age). The relative weights of these features are shown in Fig. 4.

The confusion matrix is used to describe the relationship between the real attributes of sample data and the types of classification prediction results (Figs. 5 and 6). The ROC curve is an integrated marker reflecting the false positivity rate and

Table 2 Characteristics of gastric cancer patients in the MS-L/S group and MSI-H group

Characteristics	Training set		P	Validation set		P
	MSI-H (n=30)	MS-L/S (n=60)		MSI-H (n=33)	MS-L/S (n=66)	
Age (average)	70.90 ± 8.69	65.65 ± 11.48	0.030	65.73 ± 9.82	65.11 ± 10.8	0.782
Gender			0.186			0.134
Male	20	49		20	51	
Female	10	11		13	15	
Tumor location			0.027			0.022
Cardia-fundus	5	8		6	11	
Body	3	21		5	27	
antrum	22	31		22	28	
CA199			0.922			1.000
Normal	24	50		26	51	
Abnormal	6	10		7	15	
CEA			1.000			0.782
Normal	25	51		28	53	
Abnormal	5	9		5	13	

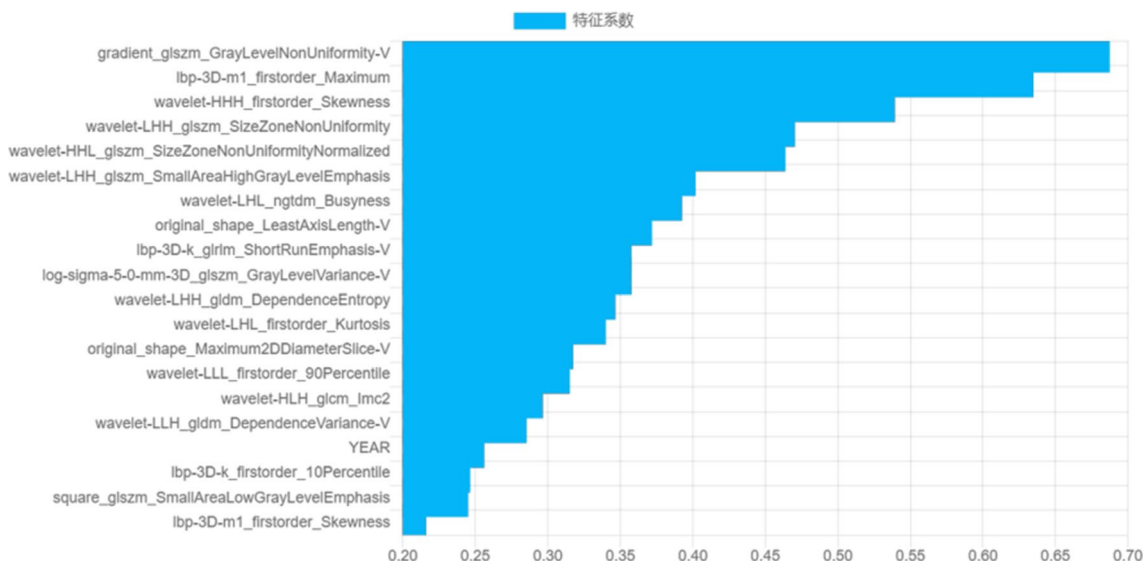


Fig. 4 The relative weights of features in the model

true positivity rate of continuous variables. The assessment markers mainly include AUC, sensitivity, specificity, and accuracy. The AUC is the main assessment marker for model performance. In this study, the ROC curve was plotted to assess the performance of the prediction model in the training set and validation set. The AUC of the training set and external validation set was 0.8228 [95% confidence interval (CI) 0.7355–0.9101] (Fig. 7) and 0.7603 [95% CI 0.6625–0.8581] (Fig. 8), respectively, and there was no significant reduction in AUC, which showed that the constructed radiomics model exhibited satisfactory generalization capabilities. The

accuracy, sensitivity, and specificity of the training dataset were 0.72, 0.63, and 0.77, respectively. The accuracy, sensitivity, and specificity of the external validation dataset were 0.67, 0.79, and 0.60, respectively.

Discussion

In this study, we constructed a non-invasive model in which clinical characteristics and radiomics features from combined CT images were used to predict the preoperative

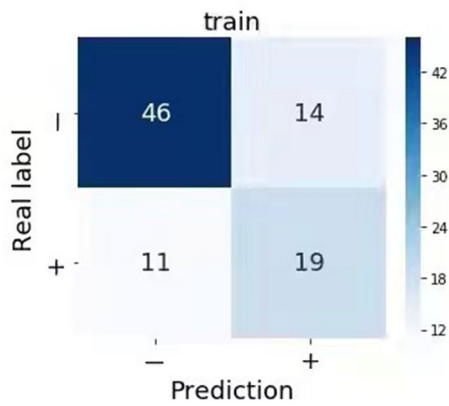


Fig. 5 Confusion matrix of the training set

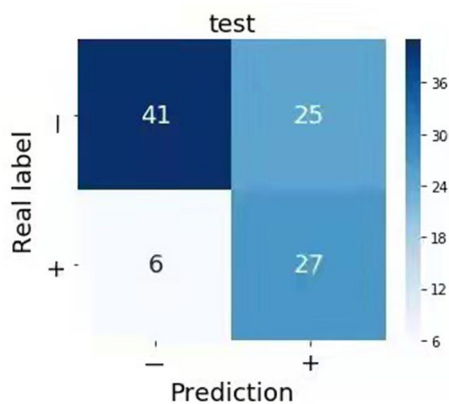


Fig. 6 Confusion matrix of the external validation set

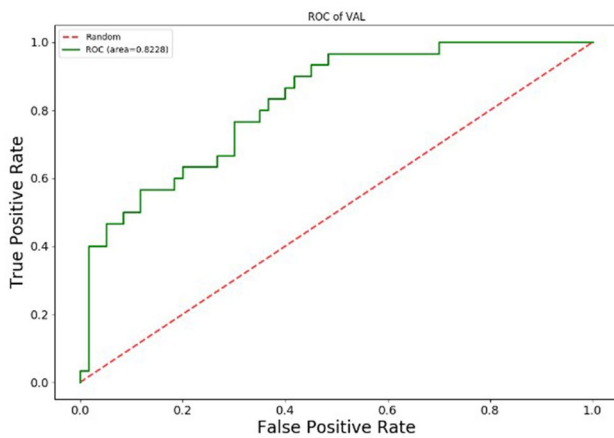


Fig. 7 ROC curve of the radiomics model in the training set

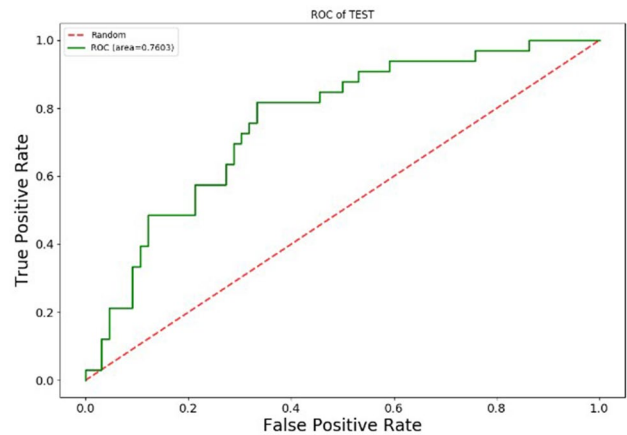


Fig. 8 ROC curve of the radiomics model in the external validation set

MSI status of gastric cancer patients. External independent datasets from many centers were used for the validation of this model, proving that this model has predictive value and

generalization capabilities, and it also has clinical application potential.

Radiomics can provide tumor phenotype and microenvironment information based on quantitative image features, such as intensity, shape, size, and texture, and microstructural changes that cannot be discerned by the naked eye can be mined. In our non-invasive model, the top two features by weight were Gray-Level Non-Uniformity (GLN) in GLSZM and the maximum of the first-order feature, and they represent the variability in gray-level intensity values in the image and the maximum gray-level intensity within the ROI. Previous studies showed that MSI-H gastric cancer is associated with tumor necrosis [25] and microvessel count (MVC) [26]. Tumor necrosis causes the density contrast differences in the tumor region to increase, while MVC differences cause differences in contrast agent uptake in the lesion after CT enhancement. These clinicopathological microstructural changes enable the use of radiomics to classify gastric cancer MSI status based on the grayscale intensity of the tumor region.

Our study found that the incidence of gastric antrum cancer in the MSI-H group was significantly higher than that in the MSI-L/S group ($p < 0.05$), which was consistent with the study of Choi et al. [27, 28]. There are different oncogenic inheritance pathways for gastric cancer in different sites, resulting in different phenotypic marker expression and biological behavior and different gene expression in tumors at different sites [29, 30]. This may be the basis for the higher incidence of gastric antrum cancer in the MSI-H group. Our study found that MSI-H gastric cancer was significantly associated with age ($p < 0.05$), as subjects with a diagnosis of MSI-H gastric cancer were older, and this was also verified by Polom et al. [5, 31]. No correlations between

MSI status and CA199 and CEA were found in the training set or the validation set.

A model developed from a single center may be dependent on the study site and instruments. Additionally, differences in site, supplier, or protocol may affect voxel intensity range, thereby affecting model generalization capabilities. In contrast, a multicenter study can provide clinical radiologic data with greater diversity, elucidate tumor heterogeneity with greater accuracy, and conforms to the developmental trend of precision medicine. Our study was a multicenter study, and the data from the largest institution were used as the training dataset, while the remaining data from the 3 institutions were used as the external validation dataset. External independent datasets from many centers were used for validation of this model. Our study results showed that our model possesses predictive value and generalization capabilities.

This study has some limitations. First, this is a retrospective study, and unavoidable selection bias is present. Second, because of the inaccurate lesion contour delineation that occurs with non-enhanced CT scans, we only extracted radiomics features from the enhanced arterial phase and portal venous phase. Third, because gastric cancer tumors are irregularly shaped, we must manually delineate the ROI, which inevitably results in some errors in tumor contour delineation. Automatic feature extraction for tumor lesions will be one of our future study directions. Finally, although we used patients from three large medical centers, our sample size remained small, and thus, a larger sample size is required for further study.

Conclusion

The radiomics model we constructed using radiomics markers from CT images and clinical characteristics has the potential to predict the MSI status of gastric cancer patients. However, additional multicenter samples are required for further validation before this model can be translated into clinical applications.

References

- Sung H, Ferlay J, Siegel RL, et al. Global Cancer Statistics 2020: GLOBOCAN Estimates of Incidence and Mortality Worldwide for 36 Cancers in 185 Countries. *CA Cancer J Clin* 2021; 71:209-249
- Cristescu R, Lee J, Nebozhyn M, et al. Molecular analysis of gastric cancer identifies subtypes associated with distinct clinical outcomes. *Nat Med* 2015; 21:449-456
- Bonneville R, Krook MA, Kautto EA, et al. Landscape of Microsatellite Instability Across 39 Cancer Types. *JCO Precis Oncol* 2017; 2017
- Liu X, Meltzer SJ. Gastric Cancer in the Era of Precision Medicine. *Cell Mol Gastroenterol Hepatol* 2017; 3:348-358
- Cai L, Sun Y, Wang K, et al. The Better Survival of MSI Subtype Is Associated With the Oxidative Stress Related Pathways in Gastric Cancer. *Front Oncol* 2020; 10:1269
- van Velzen MJM, Derks S, van Grieken NCT, Haj Mohammad N, van Laarhoven HWM. MSI as a predictive factor for treatment outcome of gastroesophageal adenocarcinoma. *Cancer Treat Rev* 2020; 86:102024
- Zhao L, Zhang J, Qu X, et al. Microsatellite Instability-Related ACVR2A Mutations Partially Account for Decreased Lymph Node Metastasis in MSI-H Gastric Cancers. *Onco Targets Ther* 2020; 13:3809-3821
- Bibeau F. The MSI status: An almost ideal marker! *Ann Pathol* 2017; 37:439-440
- Duffy MJ, Crown J. Biomarkers for Predicting Response to Immunotherapy with Immune Checkpoint Inhibitors in Cancer Patients. *Clin Chem* 2019; 65:1228-1238
- Rodriquenz MG, Roviello G, D'Angelo A, Lavacchi D, Roviello F, Polom K. MSI and EBV Positive Gastric Cancer's Subgroups and Their Link With Novel Immunotherapy. *J Clin Med* 2020; 9
- Raimondi A, Palermo F, Prisciandaro M, et al. Tremellumab and Durvalumab Combination for the Non-Operative Management (NOM) of Microsatellite Instability (MSI)-High Resectable Gastric or Gastroesophageal Junction Cancer: The Multicentre, Single-Arm, Multi-Cohort, Phase II INFINITY Study. *Cancers (Basel)* 2021; 13
- Svrcek M. Vers un screening systématique du statut MMR déficient/MSI sur toutes les biopsies de cancers de l'estomac. *Ann Pathol* 2019; 39:381-382
- Fukuda M, Yokozaki H, Shiba M, Higuchi K, Arakawa T. Genetic and epigenetic markers to identify high risk patients for multiple early gastric cancers after treatment with endoscopic mucosal resection. *J Clin Biochem Nutr* 2007; 40:203-209
- Berry P, Kotha S, Tritto G, DeMartino S. A three-tiered approach to investigating patient safety incidents in endoscopy: 4-year experience in a teaching hospital. *Endosc Int Open* 2021; 9:E1188-e1195
- Kim GH. Systematic Endoscopic Approach for Diagnosing Gastric Subepithelial Tumors. *Gut Liver* 2022; 16:19-27
- Gillies RJ, Kinahan PE, Hricak H. Radiomics: Images Are More than Pictures, They Are Data. *Radiology* 2016; 278:563-577
- Compter I, Verduin M, Shi Z, et al. Deciphering the glioblastoma phenotype by computed tomography radiomics. *Radiother Oncol* 2021; 160:132-139
- Wang W, Cao K, Jin S, Zhu X, Ding J, Peng W. Differentiation of renal cell carcinoma subtypes through MRI-based radiomics analysis. *Eur Radiol* 2020; 30:5738-5747
- Li C, Yin J. Radiomics Nomogram Based on Radiomics Score from Multiregional Diffusion-Weighted MRI and Clinical Factors for Evaluating HER-2 2+ Status of Breast Cancer. *Diagnostics (Basel)* 2021; 11
- Li Z, Zhong Q, Zhang L, et al. Computed Tomography-Based Radiomics Model to Preoperatively Predict Microsatellite Instability Status in Colorectal Cancer: A Multicenter Study. *Front Oncol* 2021; 11:666786
- Cao Y, Zhang G, Zhang J, et al. Predicting Microsatellite Instability Status in Colorectal Cancer Based on Triphasic Enhanced Computed Tomography Radiomics Signatures: A Multicenter Study. *Front Oncol* 2021; 11:687771
- Huang Z, Zhang W, He D, et al. Development and validation of a radiomics model based on T2WI images for preoperative prediction of microsatellite instability status in rectal cancer: Study Protocol Clinical Trial (SPIRIT Compliant). *Medicine (Baltimore)* 2020; 99:e19428
- Zhang W, Huang Z, Zhao J, et al. Development and validation of magnetic resonance imaging-based radiomics models for

- preoperative prediction of microsatellite instability in rectal cancer. *Ann Transl Med* 2021; 9:134
24. Zhang W, Yin H, Huang Z, et al. Development and validation of MRI-based deep learning models for prediction of microsatellite instability in rectal cancer. *Cancer Med* 2021; 10:4164–4173
 25. Kim JY, Shin NR, Kim A, et al. Microsatellite instability status in gastric cancer: a reappraisal of its clinical significance and relationship with mucin phenotypes. *Korean J Pathol* 2013; 47:28–35
 26. Miyamoto N, Yamamoto H, Taniguchi H, et al. Differential expression of angiogenesis-related genes in human gastric cancers with and those without high-frequency microsatellite instability. *Cancer Lett* 2007; 254:42–53
 27. Choi J, Nam SK, Park DJ, et al. Correlation between microsatellite instability-high phenotype and occult lymph node metastasis in gastric carcinoma. *APMIS* 2015; 123:215–222
 28. Wu MS, Lee CW, Shun CT, et al. Distinct clinicopathologic and genetic profiles in sporadic gastric cancer with different mutator phenotypes. *Genes Chromosomes Cancer* 2000; 27:403–411
 29. Chung HW, Lee SY, Han HS, et al. Gastric cancers with microsatellite instability exhibit high fluorodeoxyglucose uptake on positron emission tomography. *Gastric Cancer* 2013; 16:185–192
 30. Shah MA, Khanin R, Tang L, et al. Molecular classification of gastric cancer: a new paradigm. *Clin Cancer Res* 2011; 17:2693–2701
 31. Polom K, Marrelli D, Roviello G, et al. Molecular key to understand the gastric cancer biology in elderly patients-The role of microsatellite instability. *J Surg Oncol* 2017; 115:344–350

Publisher's Note Springer Nature remains neutral with regard to jurisdictional claims in published maps and institutional affiliations.